A Consistent Flamelet Formulation for Non-Premixed Combustion Considering Differential Diffusion Effects

H. PITSCH* and N. PETERS

Institut für Technische Mechanik, RWTH Aachen, Templergraben 64, 52056 Aachen, Federal Republic of Germany

A flamelet formulation for non-premixed combustion that allows an exact description of differential diffusion has been developed. The main difference to previous formulations is the definition of a mixture fraction variable, which is not related directly to any combination of the reactive scalars, but defined from the solution of a conservation equation with an arbitrary diffusion coefficient and appropriate boundary conditions. Using this definition flamelet equations with the mixture fraction as the independent coordinate are derived without any assumptions about the Lewis numbers for chemical species. The formulation is shown to be exact if the scalar dissipation rate is prescribed as a function of the mixture fraction. Different approximations of the scalar dissipation rate that had been derived from analytic solutions for special cases are investigated by varying the diffusion coefficient of the mixture fraction transport equation. As examples, counterflow flames of hydrogen and n-heptane, which have much larger and much smaller diffusivities than oxygen and nitrogen, are considered. It is shown that the use of equal thermal and mixture fraction diffusivities yields a sufficiently well-described flame structure and is therefore recommended for the definition of the mixture fraction diffusion coefficient. Finally, the possibility of using constant species Lewis numbers has been examined. It has been found that once an appropriate set of Lewis numbers is determined, good results are achieved over wide ranges of the parameters, such as scalar dissipation rate, pressure, and oxidizer temperature.

NOMENCLATURE

a_∞	strain rate
C	Chapman–Rubesin parameter
c_p	specific mixture heat capacity at constant pressure
c_{pi}	specific heat capacity of species i at constant pressure
D_i	diffusion coefficient of species i
D_Z	diffusion coefficient of the mixture fraction
h_i	enthalpy of species i
Le_i	Lewis number of species i
Le_Z	Lewis number of the mixture fraction
$\dot{m}_i$	chemical production rate of species i
N	number of chemical species
p	pressure
S_i	sensitivity coefficient
Sc_i	Schmidt number of species i
T	temperature
t	time
u, v	velocities in x, y-direction
$\mathbf{v}$	velocity vector
V_{iy}	diffusion velocity of species i in y-direction
V_{iy}^D	ordinary diffusion velocity of species i in y-direction
V_y^C	diffusion correction velocity in y-direction
V_{iy}^{DY}	mass fraction gradient contribution to V_{iy}^D
V_{iy}^{DW}	molecular weight gradient contribution to V_{iy}^D
V_y^{CY}	mass fraction gradient contribution to V_y^C
V_y^{CW}	molecular weight gradient contribution to V_y^C
W	mean molecular weight of the mixture
W_i	molecular weight of species i
X_i	mole fraction of species i
x, y	physical coordinates
Y_i	mass fraction of species i
Z	mixture fraction
Z_i	mass fraction of element i

Greek Symbols

β	coupling function
λ	heat conductivity

*Corresponding author.

0010-2180/98/$19.00
PII S0010-2180(98)00278-2

COMBUSTION AND FLAME 114:26–40 (1998)

Published by Elsevier Science Inc.

ν stoichiometric mass ratio
ν_i stoichiometric coefficient of species or element i
μ dynamic viscosity
ω reaction rate
ρ density
τ transformed time coordinate
χ scalar dissipation rate

Subscripts

1, F Fuel
2, Ox Oxidizer
st stoichiometric mixture

INTRODUCTION

Flamelet theory for non-premixed combustion has been used successfully for numerical predictions of turbulent combustion [1–5] and the evaluation of experimental data [6–7]. According to Refs. 9 and 10 the flamelet equations are given by

$$\rho \frac{\partial Y_i}{\partial t} - \rho \frac{\chi}{2} \frac{\partial^2 Y_i}{\partial Z^2} - \dot{m}_i = 0 \tag{1}$$

$$\rho \frac{\partial T}{\partial t} - \rho \frac{\chi}{2} \frac{\partial^2 T}{\partial Z^2} - \frac{1}{c_p} \frac{\partial p}{\partial t} + \sum_{i=1}^{N} h_i \dot{m}_i = 0. \tag{2}$$

This formulation relies on the Shvab–Zeldovich formulation of the species mass fraction and energy equations, which involves the approximation of unity Lewis numbers for all species (see, for example, Ref. 10). The Lewis numbers Le_i are defined by

$$\mathrm{Le}_i = \frac{\lambda}{\rho D_i c_p} \tag{3}$$

and represent the ratio of thermal to mass diffusivities.

Several authors have investigated the influence of nonunity Lewis numbers on turbulence–chemistry interaction [11] and on laminar flame structure using asymptotic analysis [12–15] and numerical calculations [16], reporting large changes in temperature, species profiles, and the extinction limit [16]. Cuenot et al. [15] have even shown that the adiabatic flame temperature is not necessarily a monotone function of the fuel and oxidizer Lewis numbers.

To account for differential diffusion effects, flamelet calculations often are performed using stretched counterflow diffusion flames with realistic transport properties instead of using the flamelet equations [17]. In Ref. 18 an additional equation for the mixture fraction was introduced in order to be able to plot the numerical results for counterflow diffusion flames as a function of the mixture fraction. On the other hand, when the equations are to be solved in mixture fraction space, a problem arises. Mauss et al. [19] retained nonunity Lewis numbers in the diffusion term solving the equations

$$\rho \frac{\partial Y_i}{\partial t} - \frac{\rho \chi}{2\mathrm{Le}_i} \frac{\partial^2 Y_i}{\partial Z^2} - \dot{m}_i = 0 \tag{4}$$

instead of Eq. 1. However, the assumption of unity Lewis numbers is used in the transport equation for the mixture fraction and this results in an inconsistent formulation, if Eq. 4 is combined to calculate element mass fractions and these are used to determine the mixture fraction.

The same problem arises in the evaluation of experimental results, if comparisons to flamelet calculations are made. But this can be circumvented by determining the mixture fraction from the numerical solutions with the same definition used in the evaluation of the experimental data.

The aim of this study is to derive an improved flamelet formulation for the numerical simulation of non-premixed combustion. The work focuses particularly on the definition of the mixture fraction, the effects of differential diffusion, and the modeling of the scalar dissipation rate. First, a new definition that allows the inclusion of differential diffusion effects will be given. Then, using appropriate transport models, the flamelet equations will be derived. Finally, simplifications of the transport model are discussed.

All equations are for the one-dimensional flame configuration, since then the final results are exact with respect to the transformation, rather than being the result of asymptotic approximations.

Calculations are shown for steady hydrogen/air flames, since the low Lewis number of hydrogen, $Le_{H_2} \approx 0.3$, causes nonequal diffusion effects to be pronounced. The ambient conditions of the presented test calculations are a pressure of $p = 1$ bar and fuel and air temperatures of $T_F = T_{Ox} = 300$ K. To study possible simplifications of the transport model, n-heptane is used to represent fuels with a higher Lewis number. Chemical rate constants are taken from Bollig et al. [20].

MIXTURE FRACTION

Since the early work of Burke and Schumann [21] the structure of non-premixed flames has been discussed in terms of conserved scalar variables, which are chemistry independent. These simply describe the mixing between fuel and oxidizer.

The classical definition of the mixture fraction is that of a normalized conserved scalar variable [10] employed by Burke and Schumann [21]. This is derived from a one-step overall chemical reaction $\nu_F F + \nu_{Ox} Ox \rightarrow \nu_P P$ with the reaction rate ω, where F, Ox, and P refer to fuel, oxidizer, and products, respectively.

With the operator

$$\mathcal{L} = \rho \frac{\partial}{\partial t} + \rho \mathbf{v} \cdot \nabla - \nabla \cdot (\rho D \nabla) \tag{5}$$

the Shvab–Zeldovich formulation of the transport equations for the mass fractions of fuel and oxidizer, with the same diffusivity for all species, is

$$\begin{aligned} \mathcal{L}(Y_F) &= -\nu_F W_F \omega \\ \mathcal{L}(Y_{Ox}) &= -\nu_{Ox} W_{Ox} \omega. \end{aligned} \tag{6}$$

Elimination of the reaction rate ω leads to the coupling function β

$$\mathcal{L}(\beta) \equiv \mathcal{L}\left(\frac{Y_F}{\nu_F W_F} - \frac{Y_{Ox}}{\nu_{Ox} W_{Ox}} \right) = 0. \tag{7}$$

If one considers a two-feed system [22], where feed 1 is the fuel stream and feed 2 is the oxidizer stream, the coupling function is normalized as

$$Z = \frac{\beta - \beta_2}{\beta_1 - \beta_2} \tag{8}$$

to yield a mixture fraction given by

$$\begin{aligned} Z &= \frac{\nu Y_F - Y_{Ox} + Y_{Ox,2}}{\nu Y_{F,1} + Y_{Ox,2}}, \\ \nu &= \frac{\nu_{Ox} W_{Ox}}{\nu_F W_F}. \end{aligned} \tag{9}$$

According to Eq. 8 the mixture fraction Z is a conserved variable with the properties of being unity in feed 1 and zero in feed 2.

If the chemistry is very fast and hence occurs in thin layers and the diffusivities of fuel and oxidizer are nearly the same, as for instance for methane/air mixtures, this definition can be used for the interpretation of experimental data. However, if more general chemistry is considered, fuel may first be converted to intermediate species. These intermediates can occur in broad layers, in which both fuel and oxidizer concentrations are negligibly small, and hence the mixture fraction from Eq. 9 has a constant value.

An alternative definition designed to remedy this problem is based on local element balancing [24]. If Z_i are the element mass fractions of C, H, and O and a global reaction

$$\nu_C C + \nu_H H + \nu_O O \rightarrow P, \tag{10}$$

is considered, the coupling function can be derived as

$$\mathcal{L}(\beta) \equiv \mathcal{L}\left(\frac{Z_C}{\nu_C W_C} + \frac{Z_H}{\nu_H W_H} - 2 \frac{Z_O}{\nu_O W_O} \right) = 0. \tag{11}$$

With Eq. 8 the mixture fraction is then given by

$$Z = \frac{Z_C/(\nu_C W_C) + Z_H/(\nu_H W_H) + 2(Z_{O,2} - Z_O)/(\nu_O W_O)}{Z_{C,1}/(\nu_C W_C) + Z_{H,1}/(\nu_H W_H) + 2Z_{O,2}/(\nu_O W_O)}. \tag{12}$$

Equation 12 no longer determines the local species composition, but the stoichiometric value of the mixture fraction is still preserved. The main disadvantage of this definition is that in the evaluation of experimental data all contributing species have to be known accurately. Furthermore, differential diffusion effects appear in a transport equation for the mixture fraction derived from the definition given by Eq. 12.

Other definitions of the mixture fraction, for instance an H atom balanced definition [24], have been used in the literature. These are equivalent to Eq. 12 but can have advantages in the evaluation of experimental data.

To create a formulation that considers differential diffusion, the mixture fraction has to be defined differently. The definitions according to Eqs. 9 and 12 have been shown to be inappropriate, because it is impossible to derive a conservation equation without the assumption of simple mixing. Hence, we define the mixture fraction in a two-feed system directly as a conserved scalar satisfying the transport equation

$$\rho \frac{\partial Z}{\partial t} + \rho \mathbf{v} \cdot \nabla Z - \nabla \cdot (\rho D_Z \nabla \cdot Z) = 0 \qquad (13)$$

and being zero in one feed and unity in the second feed. For this definition no assumptions about the Lewis numbers of the chemical components have been made. As a consequence, the mixture fraction no longer preserves its stoichiometric value because the mixture fraction distribution is only determined by the conservation equation and hence is uncoupled completely from the local composition. However, this is not a restriction for the resulting flamelet model, since the stoichiometric value of the mixture fraction is not required. As a constant reference value of the mixture fraction the stoichiometric value evaluated from Eq. 9 or 12 will be used.

In Eq. 13 D_Z is an arbitrary diffusion coefficient, which, for instance, can be chosen such that the Lewis number of the mixture fraction Le_Z is equal to unity.

Equation 13 also can be derived formally from an element-based definition of the mixture fraction under the assumption of unity Lewis numbers, but note that here the transport equation is the definition of the mixture fraction, and thus simple transport has not been assumed.

FLAMELET EQUATIONS

If laminar counterflow diffusion flames are considered, a one-dimensional set of equations can be derived [25] and the governing transport equations for species mass fractions Y_i and temperature T are given by

$$\rho \frac{\partial Y_i}{\partial t} + \rho v \frac{\partial Y_i}{\partial y} + \frac{\partial}{\partial y}(\rho Y_i V_{iy}) - \dot{m}_i = 0, \qquad (14)$$

$$i = 1, \ldots, N,$$

$$\rho c_p \frac{\partial T}{\partial t} + \rho v c_p \frac{\partial T}{\partial y} - \frac{\partial}{\partial y}\left(\lambda \frac{\partial T}{\partial y}\right) + \sum_{i=1}^{N} \rho Y_i V_{iy} c_{pi} \frac{\partial T}{\partial y} - \frac{\partial p}{\partial t} + \sum_{i=1}^{N} h_i \dot{m}_i = 0. \qquad (15)$$

The diffusion velocities are commonly expressed by the Curtiss–Hirschfelder approximation [26] with a correction velocity V^C accounting for mass conservation (Method III in Ref. 27)

$$V_{iy} = V_{iy}^D + V_y^C, \qquad (16)$$

where the ordinary diffusion velocities in the absence of pressure gradients and external forces are given by

$$V_{iy}^D = -\frac{1}{X_i} D_i \frac{\partial X_i}{\partial y} = \underbrace{-\frac{D_i}{Y_i}\frac{\partial Y_i}{\partial y}}_{V_{iy}^{DY}} \underbrace{-\frac{D_i}{W}\frac{\partial W}{\partial y}}_{V_{iy}^{DW}} \qquad (17)$$

and the correction velocity, determined from the mass conservation constraint $\sum_{k=1}^{N} Y_k V_{ky} = 0$, is

$$V_y^C = \sum_{k=1}^{N} \frac{Y_k}{X_k} D_k \frac{\partial X_k}{\partial y} = \underbrace{\sum_{k=1}^{N} D_k \frac{\partial Y_k}{\partial y}}_{V_y^{CY}} + \underbrace{\sum_{k=1}^{N} \frac{Y_k D_k}{W}\frac{\partial W}{\partial y}}_{V^{CW}}. \qquad (18)$$

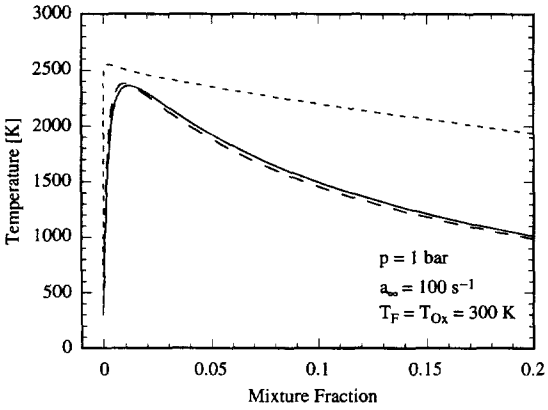

Fig. 1. Comparison of different diffusion velocity approximations in a hydrogen diffusion flame. Solid line represents use of polynary diffusion coefficients; dashed line represents use of binary diffusion coefficients. Dotted line represents a simple mixing approach with diffusion velocities approximated by Eq. 19.

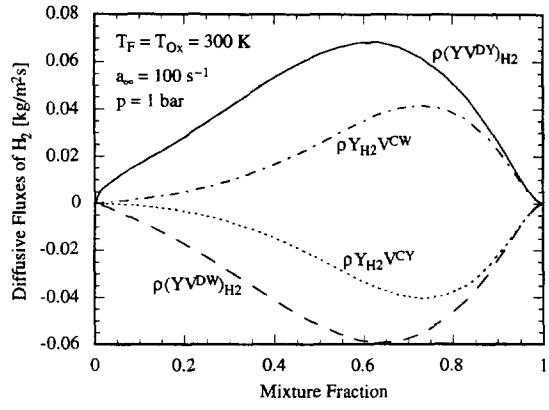

Fig. 2. Individual contributions to diffusive fluxes of the fuel in a hydrogen diffusion flame. Solid and dashed lines represent the mass fraction and molar mass dependence of ordinary diffusion; the dotted and the dash-dotted line represent respective parts of the diffusion correction.

Figure 1 demonstrates the importance of the diffusion approximation. Numerical calculations applying this approximation are compared with a more complex model using polynary diffusion coefficients (Method I in [27]). The models are in good agreement, which has already been shown by other authors [28]. Additionally, to demonstrate the necessity of an elaborated diffusion model for a general formulation, the results using a simple model for the diffusive fluxes, approximating the diffusion velocities by

$$V_{iy} = -\frac{1}{Y_i} D_i \frac{\partial Y_i}{\partial y}, \tag{19}$$

are shown in Fig. 1. This model has, for example, been employed by Smooke et al. [29] for methane flames leading to reasonable results and also is used in Eq. 4. However, for hydrogen flames the approximation yields a remarkable overprediction of the temperature and an incorrectly predicted flame location.

The individual parts of diffusive fluxes $\rho Y_{H_2} V_{H_2}$ of hydrogen, separated in the contributions from mass fraction and molecular weight gradients of ordinary diffusion and diffusion correction as given in Eqs. 17 and 18 are compared in Fig. 2, showing all of them to be in the same order of magnitude, and, hence, none to be negligible.

Introducing the diffusion velocity given by Eq. 16 in Eqs. 14 and 15 yields

$$\rho \frac{\partial Y_i}{\partial t} + \rho v \frac{\partial Y_i}{\partial y} - \frac{\partial}{\partial y}\left(\rho D_i \frac{Y_i}{X_i}\frac{\partial X_i}{\partial y}\right) + \sum_{k=1}^{N} \frac{\partial}{\partial y}\left(\rho Y_i D_k \frac{Y_k}{X_k}\frac{\partial X_k}{\partial y}\right) - \dot{m}_i = 0 \tag{20}$$

and

$$\rho c_p \frac{\partial T}{\partial t} + \rho v c_p \frac{\partial T}{\partial y} - \frac{\partial}{\partial y}\left(\lambda \frac{\partial T}{\partial y}\right) - \sum_{i=1}^{N} \rho D_i \frac{Y_i}{X_i}\frac{\partial X_i}{\partial y}(c_{pi} - c_p)\frac{\partial T}{\partial y} - \frac{\partial p}{\partial t} + \sum_{i=1}^{N} h_i \dot{m}_i = 0. \tag{21}$$

Equations 20 and 21 are solved with a continuity and a momentum equation. In these equations the strain rate appears as an independent parameter, which for planar potential flow is defined as $a_\infty = \partial u_\infty / \partial x$. Since ρv from the convective terms in Eqs. 20 and 21 will in the following be eliminated by Eq. 13, continuity and momentum equations are not needed here, and the influence of the strain rate is included in the scalar dissipation rate, which will be defined below. In the following derivation of the flamelet equations the mixture fraction definition given by Eq. 13 is used. The results obtained by solving the flamelet equations are compared

with the solution of Eqs. 20 and 21. Therefore, Eq. 13 is solved with these equations as a passive scalar.

Following Refs. 8 and 9, a flame attached coordinate system is introduced in Eqs. 20 and 21 by replacing the spatial coordinate y with the mixture fraction Z and using $\tau = t$ as the other independent variable.

Applying the formal transformation rules

$$\frac{\partial}{\partial t} = \frac{\partial}{\partial \tau} + \frac{\partial Z}{\partial t}\frac{\partial}{\partial Z}$$

$$\frac{\partial}{\partial y} = \frac{\partial Z}{\partial y}\frac{\partial}{\partial Z} \tag{22}$$

to Eqs. 20 and 21 and using Eq. 13, Eq. 3 and the relation

$$\frac{\partial}{\partial y}\left(\phi D_Z \frac{\partial Z}{\partial y}\right) = \frac{\partial Z}{\partial y}\frac{\partial}{\partial Z}\left(\phi D_Z \frac{\partial Z}{\partial y}\right) = \frac{1}{4}\left[\frac{\partial \phi \chi}{\partial Z} + \rho\chi \mathrm{Le}_Z \frac{c_p}{\lambda}\frac{\partial}{\partial Z}\left(\frac{\phi\lambda}{\rho c_p \mathrm{Le}_Z}\right)\right] \tag{23}$$

for an arbitrary scalar quantity ϕ leads to the flamelet equations

$$\rho\frac{\partial Y_i}{\partial \tau} - \underbrace{\frac{\rho\chi}{2}\frac{\mathrm{Le}_Z}{\mathrm{Le}_i}\frac{\partial^2 Y_i}{\partial Z^2}}_{\text{2. diffusion } V_{iy}^{DY}} - \dot{m}_i$$

$$\underbrace{-\frac{\rho\chi}{2}\frac{\mathrm{Le}_Z}{\mathrm{Le}_i}\frac{Y_i}{W}\frac{\partial^2 W}{\partial Z^2}}_{\text{4. diffusion } V_{iy}^{DW}} + \underbrace{\frac{\rho\chi}{2}\sum_{k=1}^{N}\left(\frac{\mathrm{Le}_Z}{\mathrm{Le}_k}Y_i\frac{\partial^2 Y_k}{\partial Z^2} + \frac{Y_i}{W}Y_k\frac{\mathrm{Le}_Z}{\mathrm{Le}_k}\frac{\partial^2 W}{\partial Z^2}\right)}_{\text{5. diffusion correction } V_y^{CY} + V_y^{CW}}$$

$$\underbrace{-\frac{1}{4}\left[2\rho\chi\frac{\partial}{\partial Z}\left(\frac{\mathrm{Le}_Z}{\mathrm{Le}_i}\right) + \left(\frac{\mathrm{Le}_Z}{\mathrm{Le}_i} - 1\right)\left(\frac{\partial \rho\chi}{\partial Z} + \rho\chi\mathrm{Le}_Z\frac{c_p}{\lambda}\frac{\partial}{\partial Z}\left(\frac{\lambda}{c_p\mathrm{Le}_Z}\right)\right)\right]\frac{\partial Y_i}{\partial Z}}_{\text{6. differential diffusion } V_{iy}^{DY}}$$

$$\underbrace{-\frac{1}{4}\left[2\rho\chi\frac{Y_i}{W}\frac{\partial}{\partial Z}\left(\frac{\mathrm{Le}_Z}{\mathrm{Le}_i}\right) + \frac{\mathrm{Le}_Z}{\mathrm{Le}_i}\left(\frac{\partial}{\partial Z}\left(\rho\chi\frac{Y_i}{W}\right) + \rho\chi\mathrm{Le}_Z\frac{c_p}{\lambda}\frac{\partial}{\partial Z}\left(\frac{\lambda}{c_p\mathrm{Le}_Z}\frac{Y_i}{W}\right)\right)\right]\frac{\partial W}{\partial Z}}_{\text{7. differential diffusion } V_{iy}^{DW}}$$

$$\underbrace{+\frac{1}{4}\sum_{k=1}^{N}\left[2\rho\chi Y_i\frac{\partial}{\partial Z}\left(\frac{\mathrm{Le}_Z}{\mathrm{Le}_k}\right) + \frac{\mathrm{Le}_Z}{\mathrm{Le}_k}\left(\frac{\partial}{\partial Z}(\rho\chi Y_i) + \rho\chi\mathrm{Le}_Z\frac{c_p}{\lambda}\frac{\partial}{\partial Z}\left(\frac{\lambda}{c_p\mathrm{Le}_Z}Y_i\right)\right)\right]\frac{\partial Y_k}{\partial Z}}_{\text{8. differential diffusion } V_y^{CY}}$$

$$\underbrace{+\frac{1}{4}\sum_{k=1}^{N}\left[2\rho\chi\frac{Y_iY_k}{W}\frac{\partial}{\partial Z}\left(\frac{\mathrm{Le}_Z}{\mathrm{Le}_k}\right) + \frac{\mathrm{Le}_Z}{\mathrm{Le}_k}\left(\frac{\partial}{\partial Z}\left(\rho\chi\frac{Y_i}{W}Y_k\right) + \rho\chi\mathrm{Le}_Z\frac{c_p}{\lambda}\frac{\partial}{\partial Z}\left(\frac{\lambda}{c_p\mathrm{Le}_Z}\frac{Y_iY_k}{W}\right)\right)\right]\frac{\partial W}{\partial Z}}_{\text{9. differential diffusion } V_y^{CW}} = 0 \tag{24}$$

and

$$\rho\frac{\partial T}{\partial \tau}-\underbrace{\frac{\rho\chi}{2}\mathrm{Le}_Z\frac{\partial^2 T}{\partial Z^2}-\frac{\rho\chi}{2}\frac{\mathrm{Le}_Z}{c_p}\frac{\partial c_p}{\partial Z}\frac{\partial T}{\partial Z}}_{\text{2. + 3. heat conduction}}-\frac{1}{c_p}\frac{\partial p}{\partial \tau}+\frac{1}{c_p}\sum_{i=1}^{N}h_i\dot{m}_i$$

$$\underbrace{-\frac{1}{4}\left[2\rho\chi\frac{\partial \mathrm{Le}_Z}{\partial Z}+(\mathrm{Le}_Z-1)\left(\frac{\partial \rho\chi}{\partial Z}+\rho\chi\mathrm{Le}_Z\frac{c_p}{\lambda}\frac{\partial}{\partial Z}\left(\frac{\lambda}{c_p\mathrm{Le}_Z}\right)\right)\right]\frac{\partial T}{\partial Z}}_{\text{6. convection by nonunity mixture fraction Lewis number}}$$

$$\underbrace{+\sum_{i=1}^{N}\frac{\rho\chi}{2}\frac{\mathrm{Le}_Z}{\mathrm{Le}_i}\left(\frac{\partial Y_i}{\partial Z}+\frac{Y_i}{W}\frac{\partial W}{\partial Z}\right)\left(1-\frac{c_{pi}}{c_p}\right)\frac{\partial T}{\partial Z}}_{\text{7. enthalpy flux}}=0. \tag{25}$$

In these equations the scalar dissipation rate χ has been introduced as

$$\chi=2D_Z\left(\frac{\partial Z}{\partial y}\right)^2. \tag{26}$$

The differential equations (Eqs. 24 and 25) describe the instantaneous local structure of the flame sheet, still accounting for nonequilibrium by stretch and differential diffusion. The derivatives of the molar fractions are expressed in terms of the mass fractions and the molecular weight of the mixture to point out the differences to the flamelet equations given by Eqs. 2 and 4. These equations still appear in the first three terms of Eq. 24 and terms 1, 2, 4, and 5 of Eq. 25, if the mixture fraction Lewis number Le_Z is assumed to be unity. Since all transported scalars, mixture fraction, species mass fractions, and the temperature are subject to the same convective transport, the convective terms appearing in Eqs. 20 and 21 disappear. The additional terms in Eqs. 24 and 25 describe the flux of species mass fractions and temperature relative to the mixture fraction due to different diffusive transport.

In the species mass fractions equation the terms appearing in addition to Eq. 4 result from the model for the molecular transport of the chemical components, which is more complex than that for the mixture fraction in Eq. 13. The fifth term in Eq. 24 includes the diffusion correction corresponding to the second and fourth term. The sixth term is formally a convection term and accounts for the different diffusion velocities of the mixture fraction and the species mass fractions. The seventh term is the corresponding contribution from the molecular weight derivative according to the last term of Eq. 17. Term 8 and 9 are the diffusion corrections of term 6 and 7.

In the energy equation given in Eq. 25, the sixth term vanishes if Le_Z is assumed to be unity and only the enthalpy flux term and a term accounting for the spatial derivative of the heat capacity remain in addition to Eq. 2. The latter results from the different form of the diffusion terms of the energy and the mixture fraction equation.

To illustrate the effect of differential diffusion, the diffusion correction will be neglected and unity mixture fraction Lewis number, constant but nonunity species Lewis numbers, constant ρD_Z, and constant molecular weight of the mixture are assumed. Then, Eq. 24 reduces to

$$\rho\frac{\partial Y_i}{\partial \tau}-\frac{\rho\chi}{2\mathrm{Le}_i}\frac{\partial^2 Y_i}{\partial Z^2}-\dot{m}_i+\frac{1}{4}\left(1-\frac{1}{\mathrm{Le}_i}\right)\cdot\frac{\partial \rho\chi}{\partial Z}\frac{\partial Y_i}{\partial Z}=0. \tag{27}$$

The only difference between Eq. 27 and Eq. 4 is the fourth term in Eq. 27, which is a convection term describing the flux of species i against the mixture fraction with the convection velocity

$$\frac{1}{4\rho}\left(1-\frac{1}{\mathrm{Le}_i}\right)\frac{\partial \rho\chi}{\partial Z}. \tag{28}$$

It will be shown later that this term is not the dominating contribution of the additional terms appearing in Eq. 24. However, it will be dis-

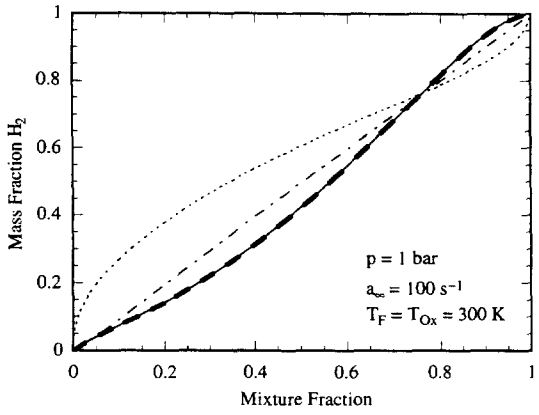

Fig. 3. H_2 mass fraction distribution in hydrogen diffusion flame from solution of flamelet equations in Eqs. 24 and 25 (bold long dashed line) compared with results from the counterflow diffusion flame (solid line). Solutions of simplified flamelet equations are represented by dotted line for convection term included (Eq. 27) and by dash-dotted line for convection term excluded (Eq. 4).

cussed exemplarily to explain the influence of these terms.

In hydrogen flames the density does not vary much in the rich part and $\rho\chi$ closely follows χ, which can be described by a bell-shaped curve between $Z = 0$ and $Z = 1$. The Lewis number of hydrogen is less than one, and hence the convection velocity is negative for small values of the mixture fraction and positive for large values of the mixture fraction. The effects of the convection term are shown in Figs. 3 and 4, where the results obtained using the simplified flamelet equations including the convection term in Eq. 27 are compared with the results of

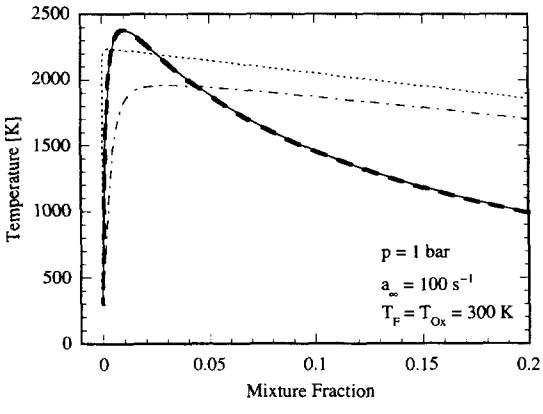

Fig. 4. Temperature distribution in hydrogen diffusion flame. See Fig. 3 for further explanation.

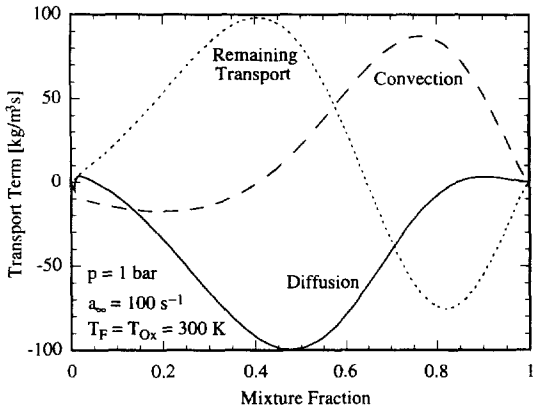

Fig. 5. Evaluation of individual terms of Eq. 24 in hydrogen diffusion flame. Diffusion term (terms 2–4) is given by the solid line, convection term (term 5) by dashed line, and remaining transport terms (terms 6–8) by dotted line.

the flamelet equations without the convection term in Eq. 4 and to the results of the exact flamelet equations given by Eq. 24.

The convective transport causes an increased hydrogen mass fraction for small values of Z and a decreased mass fraction for large Z. The temperature distribution given in Fig. 4 reveals that the flame is shifted markedly to the lean side. However, comparison with the solution of the exact flamelet equations shows that the convection term is even overcompensated by other effects. This is also shown in Fig. 5, where from the solution of the exact hydrogen mass fraction flamelet equation given in Eq. 24 the diffusion term (terms 2, 4, 5) is compared with the convection term (term 6) and the remaining transport terms (terms 7–9). Obviously, in contrast to term 6, terms 7–9 are positive at the lean side and negative for higher values of Z. Since chemical reactions are small outside a thin reaction zone at approximately $Z = 0.01$, terms 6–9 have to be balanced by the diffusion terms and are therefore of the same order of magnitude.

Figure 6 shows the individual contributions of terms 6–9 from the solution of the hydrogen mass fraction equation given in Eq. 24 revealing all terms to be of comparable magnitude for $Z > 0.8$. Terms 7 and 9 yield the most important contributions for $0.2 < Z < 0.8$ and in the reaction zone term 6 is predominant.

In these calculations the mixture fraction Lewis number has been chosen as unity so that the

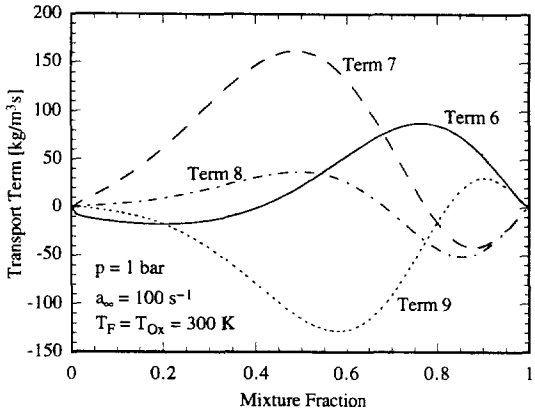

Fig. 6. Individual contributions of newly appearing transport terms in flamelet equation for the chemical components given in Eq. 24 in hydrogen diffusion flame.

ratio of fuel and mixture fraction Lewis number is approximately $Le_{H_2}/Le_Z \approx 0.3$. By increasing the Lewis number ratio to unity, term 6 disappears. For larger values of the Lewis number ratio the convection velocity in Eq. 28 changes direction and since terms 7–9 vanish for large species Lewis numbers, term 6 becomes dominant.

The most important feature of the flamelet equations given in Eqs. 24 and 25 is that they are exact with respect to the transformation and that, except for the validity of Eqs. 20 and 21, no further assumptions are made. Hence, if the scalar dissipation rate is known, Eqs. 24 and 25 yield exactly the same results as Eqs. 20 and 21. To prove this, Figs. 3 and 4 show hydrogen mass fraction and temperature profiles from the solution of Eqs. 20 and 21 and Eqs. 24 and 25, respectively. For the solution of the flamelet equations, the applied scalar dissipation rate has been evaluated from the solution of the counterflow configuration using Eq. 26. The profiles do not even show numerical differences, if central differences are used in the numerical discretization scheme.

SCALAR DISSIPATION RATE

Applying the universal coordinate transformation given by Eq. 22, the spatial coordinate is replaced by the mixture fraction. Since all scalars are transported convectively with the same mean flow velocity, temperature and species mass fractions move with the mixture fraction and the convective terms in Eqs. 20 and 21 vanish with the transformation. Diffusive fluxes arising from spatial gradients are described as a function of the gradients of the mixture fraction Z, and hence the influence of the flow field on the flamelet structure is represented completely by the scalar dissipation rate χ.

In flamelet calculations for turbulent flows often flamelet libraries are used. These libraries are computed in advance and are assumed to be independent of the flow. The scalar dissipation rate can therefore not be taken from the flow field calculation, but has to be introduced as a scalar parameter. Then, the mixture fraction dependence of the scalar dissipation rate, which is required to compute the flamelet libraries, has to be modeled.

It was shown in Ref. 8 from the analytic solutions of laminar counterflow diffusion flames and for the unsteady mixing layer that for constant density and unity ratio of mixture fraction Schmidt number Sc_Z and Chapman-Rubesin parameter C, which are defined as

$$Sc_Z = \frac{\mu}{\rho D_Z} \quad \text{and} \quad C = \frac{\rho\mu}{(\rho\mu)_\infty}, \tag{29}$$

the scalar dissipation rate can be expressed as a function of the mixture fraction

$$\chi(Z) = \frac{a_\infty}{\pi} \exp\{-2[\mathrm{erfc}^{-1}(2Z)]^2\}, \tag{30}$$

where erfc^{-1} stands for the inverse of the complementary error function.

From the asymptotic analysis of counterflow diffusion flames Kim et al. [32] formulated an improved relation for variable density, but still $Sc_Z = 1$ and $C = 1$. Their scalar dissipation rate that will be used in the following discussions is given by

$$\chi(Z) = \frac{a_\infty}{4\pi} \frac{3(\sqrt{\rho_\infty/\rho} + 1)^2}{2\sqrt{\rho_\infty/\rho} + 1} \cdot \exp\{-2[\mathrm{erfc}^{-1}(2Z)]^2\}. \tag{31}$$

In Figs. 7 and 8 the results of Eqs. 30 and 31 are compared with the scalar dissipation rate evaluated from the solution of the mixture fraction transport equation given by Eq. 13. The maximum flame temperatures in counterflow diffusion flames as a function of the scalar

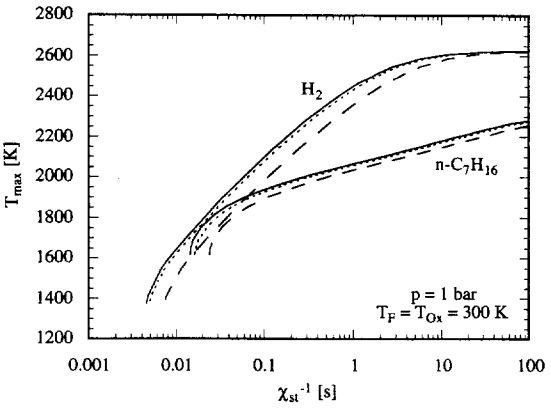

Fig. 7. Comparison of different approximations for scalar dissipation rate at Z_{st}. Solid lines represent χ_{st} calculated with transport equation (Eq. 13); dashed and dotted lines represent χ_{st} from Eqs. 30 and 31, respectively.

dissipation rate χ_{st} are shown in Fig. 7. Here, χ_{st} denotes the scalar dissipation rate of a stoichiometric mixture fraction Z_{st} according to the mixture fraction definitions, in Eqs. 9 or 12. As pointed out earlier, the stoichiometric mixture fraction determined by the solution of Eq. 13 is not a constant and can therefore not be used as a constant reference value in the presented flamelet formulation.

The scalar dissipation rate evaluated from the solution of the mixture fraction transport equation using Eq. 13 is the definition of χ and is

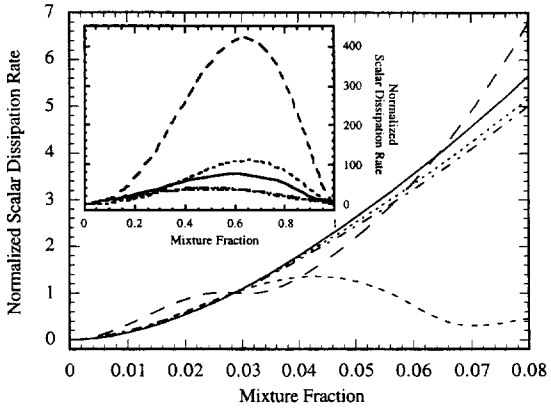

Fig. 8. Mixture fraction dependence of scalar dissipation rate calculated using transport equation (Eq. 13, solid line) compared with evaluations using the fuel mass-based Z-definition (Eq. 9, short dashed line), the element mass-based Z-definition (Eq. 12, long dashed line), and formulas from analytic solutions given by Eq. 30 (dash-dotted line) and Eq. 31 (dotted line).

represented by the full lines. Additionally, the stoichiometric scalar dissipation rate has been calculated from the strain rate by using Eqs. 30 and 31, represented by the dashed and dotted lines, respectively. Both formulas describe the trends quite well, while Eq. 31 is shown to be a reasonably accurate approximation even for the absolute values of the scalar dissipation rate.

The mixture fraction dependence of the scalar dissipation rate in a hydrogen diffusion flame, again calculated by the solution of Eqs. 13, 30, and 31, is shown in Fig. 8. The scalar dissipation rate has been made nondimensional using χ_{st}, which is evaluated at Z_{st} according to Eqs. 9 or 12. Because of the almost constant density throughout the rich part of the flame, the results of Eqs. 30 and 31 differ only slightly, both yielding good approximations in the reactive layer. In general, the approximations tend to underpredict the scalar dissipation rate. The reason is that the underlying assumption of $Sc_Z = C = 1$ implies that in the derivation of Eq. 31

$$\rho^2 D_Z = (\rho\mu)_\infty. \tag{32}$$

If in the definition of the mixture fraction given by Eq. 13 the diffusion coefficient is determined from a unity mixture fraction Lewis number, $\rho^2 D_Z$ depends on the temperature. Under the simplifying assumptions of constant molecular weight of the mixture and $\lambda/c_p \sim T^{1.3}$ [29] this can be approximated by

$$\rho^2 D_Z \sim T^{-0.3}. \tag{33}$$

This shows that Eq. 32 is a reasonable assumption because of the weak temperature dependence, but Eq. 31 will underpredict the scalar dissipation rate, since Eq. 33 shows that if $\rho^2 D_Z$ is evaluated in the oxidizer stream with the assumption $C = 1$ it is an upper bound of the mixture fraction diffusivity, which leads to lower mixture fraction gradients.

Figure 8 additionally demonstrates the influence of the definition of the mixture fraction by showing the scalar dissipation rate evaluated with the mixture fraction definitions from Eqs. 9 and 12. Although χ defined by the mixture fraction transport equation (see Eq. 13) and from the analytic solutions given by Eqs. 30 and 31 are described by bell-shaped functions, the evaluations of the scalar dissipation rate using

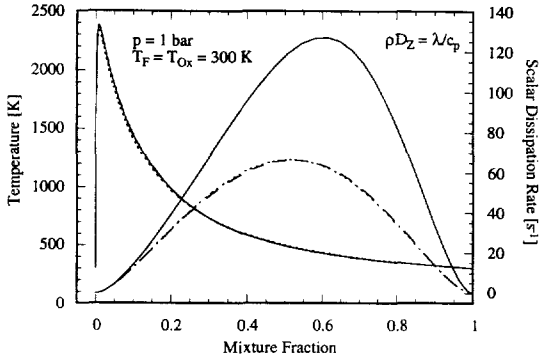

Fig. 9. Scalar dissipation rate and temperature distribution in hydrogen diffusion flame for $\rho D_Z = \lambda/c_p$. Solid lines represent the counterflow diffusion flame; dashed lines represent flamelet solution with scalar dissipation rate approximated by Eq. 31 and dotted line flamelet solution with assumption of constant Lewis numbers for chemical components.

the fuel mass definition (see Eq. 9) or the element mass definition of the mixture fraction (see Eq. 12) show an additional local minimum for small values of Z. This leads to a completely different behavior of the scalar dissipation rate in the reaction zone. Also this has been found experimentally, for instance by Nandula et al. [6] and Chen et al. [7].

In the presented flamelet formulation, the scalar dissipation rate is the only unknown that has to be modeled. Figures 9 and 10 show calculations for a hydrogen and an n-heptane diffusion flame, respectively, using Eqs. 24 and 25 with the scalar dissipation rate approximated by Eq. 31, represented by the dashed lines, compared with the solution of Eqs. 20, 21, and

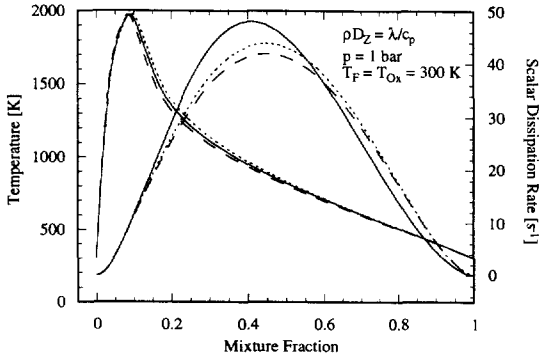

Fig. 10. Scalar dissipation rate and temperature distribution in n-heptane diffusion flame for $\rho D_Z = \lambda/c_p$. See Fig. 9 for further explanation.

13, given by the full lines. The diffusion coefficient in Eq. 13 has been chosen from $\rho D_Z = \lambda/c_p$, from the assumption $\mathrm{Le}_Z = 1$. The scalar dissipation rate is well approximated around the reaction zone for both fuels. However, for $Z > 0.2$ it is strongly underestimated for the hydrogen flame and is shifted to the rich side for the n-heptane flame. The resulting error in the maximum flame temperature due to the modeled scalar dissipation rate is shown in Fig. 9 to be approximately 35 K for the hydrogen flame. For the n-heptane flame the maximum temperatures, depicted in Fig. 10, are almost identical, but the flame is slightly shifted to the lean side.

Although a constant, and especially a unity, Lewis number of the mixture fraction has some advantages, it could be worthwhile to consider the definition $\rho^2 D_Z = (\rho\mu)_\infty$ from Eq. 32 in the equation for the mixture fraction, since then Eq. 31 is an exact solution of the mixture fraction equation with respect to diffusive transport. The only approximation that has to be applied is for the convective mass flux ρv, which is determined from the asymptotic analysis of counterflow diffusion flames [32]. Then, the Lewis number of the mixture fraction Le_Z is

$$\mathrm{Le}_Z = \frac{\rho}{(\rho\mu)_\infty}\frac{\lambda}{c_p}. \tag{34}$$

Indeed, using constant $\rho^2 D_Z$ in Eq. 13 and introducing the mixture fraction Lewis number according to Eq. 34 in Eqs. 24 and 25, the scalar dissipation rate given by Eq. 31 is a much better approximation for both the hydrogen and the n-heptane diffusion flame. This is shown in Figs. 11 and 12, where again the scalar dissipation rate from the solution of the mixture fraction transport equation in Eq. 13, given by the full lines, is compared with the analytic solution in Eq. 31, given by the dashed lines. The maximum of the scalar dissipation rate is still underpredicted, but the overall shape is in much better agreement in both figures. However, this does not lead to a significant improvement of the solution. The comparison of the resulting temperature profiles shows those for the hydrogen flame to be slightly improved with an error in the maximum temperature of approximately 25 K, but in the n-heptane flame an underprediction of the scalar dissipation rate of approxi-

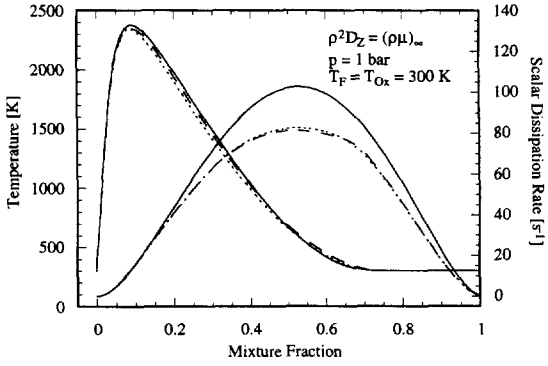

Fig. 11. Scalar dissipation rate and temperature distribution in hydrogen diffusion flame for $\rho D_Z = (\rho\mu)_\infty/\rho$ from $Sc_Z = C = 1$. See Fig. 9 for further explanation.

mately 15% for $Z < 0.05$ causes a shift of the temperature profile to the lean. In the following we will therefore fix the arbitrary diffusion coefficient in the mixture fraction definition by $\rho D_Z = \lambda/c_p$ from the assumption $Le_Z = 1$ in the definition of the mixture fraction.

The maximum flamelet temperatures in hydrogen and n-heptane diffusion flames are shown in Fig. 13. Solutions from counterflow diffusion flames indicated by the solid lines are compared with flamelet solutions with the scalar dissipation rate approximated by Eq. 31 given by the dashed lines. The agreement for n-heptane is very good, the errors for the hydrogen flames caused by the approximation of the scalar dissipation rate are approximately 25 K throughout the whole parameter range. The scalar dissipation rate at extinction is well predicted for both fuels.

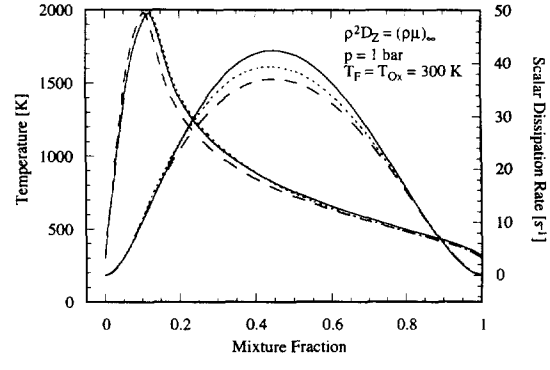

Fig. 12. Scalar dissipation rate and temperature distribution in n-heptane diffusion flame for $\rho D_Z = (\rho\mu)_\infty/\rho$ from $Sc_Z = C = 1$. See Fig. 9 for further explanation.

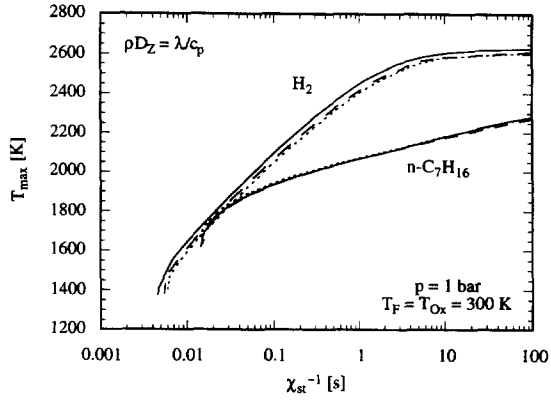

Fig. 13. Maximum flame temperature as a function of scalar dissipation rate at Z_{st} for hydrogen and n-heptane diffusion flames with $\rho D_Z = \lambda/c_p$. See Fig. 9 for further explanation.

CONSTANT LEWIS NUMBER APPROACH

The use of constant Lewis numbers for the chemical components has some advantages in the present formulation, for example all Z-derivatives of the species Lewis numbers in Eq. 24 vanish. The main benefit, however, is that the very expensive calculation of the binary diffusion coefficients, which are required to evaluate nonconstant Lewis numbers for the chemical components, can be omitted.

Although the fuel Lewis numbers in the investigated hydrogen and n-heptane diffusion flames vary over the mixture fraction by a factor of approximately 2, the reasonable results from calculations using constant Lewis numbers given, for example, in Figs. 9–13, represented by the dotted lines, indicate that the constant Lewis number approach for chemical species can be applied with an acceptable error. However, the results depend strongly on the particular choice of the Lewis numbers. Therefore, in this section a new approach is suggested for the determination of the values for the constant Lewis numbers from a flamelet solution with detailed transport, and the applicability to different parameter and boundary conditions is investigated.

The effects of the particular choice of the species Lewis numbers on the flame structure are examined by employing a sensitivity analysis. The results for hydrogen and n-heptane diffusion flames are depicted in Figs. 14 and 15. Figure 15 includes only species with a sensitivity

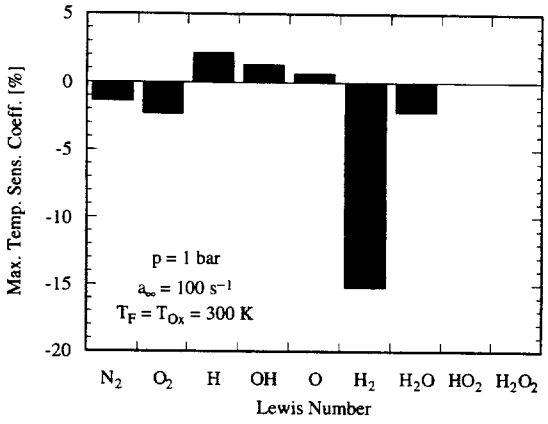

Fig. 14. Sensitivity analysis of influence of species Lewis numbers on maximum temperature in hydrogen diffusion flame.

coefficient larger than ±1%. The sensitivity coefficients are defined as

$$S_i = \frac{\mathrm{Le}_i}{T_{\max}} \frac{\partial T_{\max}}{\partial \mathrm{Le}_i}. \tag{35}$$

In the hydrogen flame the Lewis number of the fuel is shown to have a strong impact on the flamelet structure, since it determines the flame location, whereas the Lewis numbers of the remaining species have much smaller sensitivity coefficients. In *n*-heptane diffusion flames the oxygen molecule has the highest sensitivity coefficient. Also, the fuel is shown to have a strong influence on the temperature. Since *n*-heptane is converted completely and replaced by intermediates at approximately $Z = 0.2$, the Lewis numbers of these also influence the temperature. In particular $\mathrm{Le}_{C_2H_2}$ has a sensitivity comparable with the fuel Lewis number.

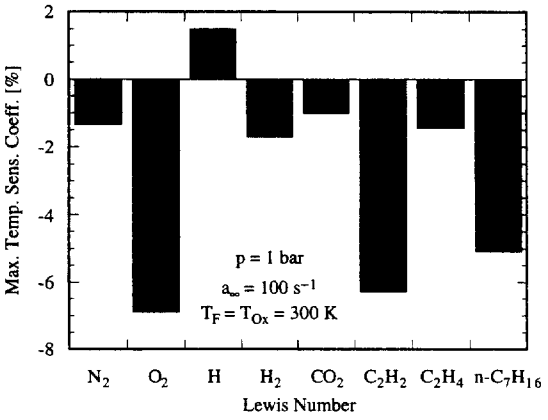

Fig. 15. Sensitivity analysis of influence of species Lewis numbers on maximum temperature in *n*-heptane diffusion flame.

Since the chemical conversion of more complex fuel molecules to combustion products occurs in several separated consumption layers, the constant Lewis numbers cannot be determined at one certain location in the flame, such as for instance at the stoichiometric mixture or the point of maximum flame temperature. Instead, the Lewis numbers of the chemical components are evaluated at the point of maximum consumption rate. The Lewis numbers of the final combustion products, CO_2 and H_2O, are evaluated at the point of maximum formation rate. For inert species, in our examples the N_2 molecule, the value at the point of maximum flame temperature has been used. This approach leads to very good results for hydrogen flames; however, for *n*-heptane flames the flame location is shifted to the rich side and the predicted temperature is too low. Considering the results from the sensitivity analysis in Fig. 15 this indicates that the Lewis number of molecular oxygen, *n*-heptane, or acetylene is too high. For molecular oxygen, the Lewis number at the maximum consumption rate is already the smallest possible choice between pure air and oxygen consumption. The acetylene Lewis number, as well as the Lewis numbers of other intermediates, hardly vary between formation and consumption because of the thin reaction layers. Hence, only the fuel Lewis number, which varies from 1.1 to 1.9 between pure fuel and maximum consumption, can be used to adjust the flame position and thereby the temperature. Here, a value of $\mathrm{Le}_{C_7H_{16}} = 1.3$ has been used.

The constant values of the Lewis numbers applied in this paper are given in Table 1 for species with a sensitivity coefficient $S_i > 1\%$. This approach leads to satisfying results, which are given by the dotted lines in Figs. 9–12 as a function of the mixture fraction and in Fig. 13 as the maximum temperature as a function of the scalar dissipation rate. The calculations have been performed using the approximation for the scalar dissipation rate from Eq. 31. The good agreement in all cases shows that for an appropriate choice of Lewis numbers the flame struc-

TABLE 1

Lewis Numbers of Species with Sensitivity Coefficients $S_i > 1\%$

	H_2/air	n-C_7H_{16}/air
N_2	1.32	0.978
O_2	1.10	0.989
H	0.175	0.165
OH	0.747	
H_2	0.313	0.275
H_2O	0.817	
CO_2		1.27
C_2H_2		1.18
C_2H_4		1.17
n-C_7H_{16}		1.30

ture, here only represented by the temperature, is well predicted over a wide range of scalar dissipation rates.

To examine the universal applicability of a set of constant species Lewis numbers determined under certain conditions, the pressure has been varied up to 20 bar and the oxidizer temperature up to 800 K. The results are compared with detailed transport flamelet calculations in Figs. 16 and 17. These show that the appropriate choice of the values for the constant species Lewis numbers is independent of the flame conditions.

SUMMARY AND CONCLUSIONS

In the present study, a flamelet formulation for non-premixed combustion has been presented,

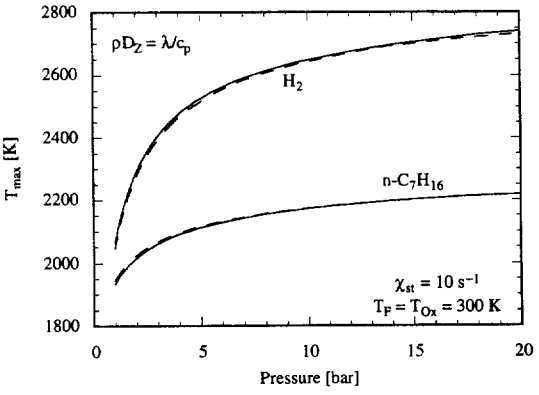

Fig. 16. Pressure dependence of maximum flame temperature for $\rho D_Z = \lambda/c_p$ and scalar dissipation rate approximated by Eq. 31 using detailed transport (solid lines) compared with constant species Lewis number approach (dashed lines).

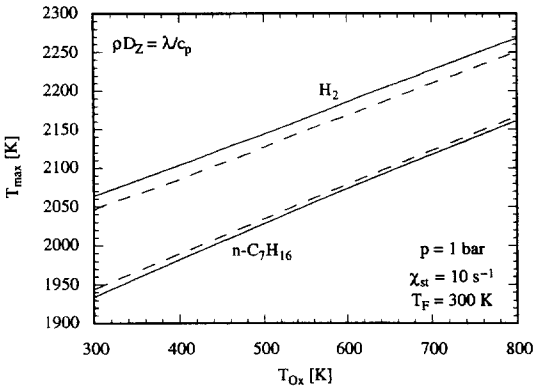

Fig. 17. Oxidizer temperature dependence of maximum flame temperature for $\rho D_Z = \lambda/c_p$ and scalar dissipation rate approximated by Eq. 31 using detailed transport (solid lines) compared with constant species Lewis number approach (dashed lines).

which allows an exact description of differential diffusion. The key to this formulation is the definition of the mixture fraction as a conserved scalar, which is only determined by the solution of a transport equation and appropriate boundary conditions. The diffusion coefficient of the transport equation is arbitrary and has been chosen to be equal to the thermal diffusivity. In this definition, the mixture fraction does not represent a combination of element mass fractions, and in particular, the stoichiometric value of the mixture fraction is not a constant. However, both consequences do not lead to strong restrictions for practical applications, because the mixture fraction as defined by Eq. 12 can always be obtained from the solution.

Using the mixture fraction as the new independent coordinate, the flamelet equations for the evolution of the chemical components and the temperature can be derived by the transformation of the governing equations, without any assumption about the Lewis numbers of the chemical species. The transformation has been shown to be exact, if the scalar dissipation rate is calculated as a function of the mixture fraction from the full set of fluid dynamic equations.

In the application of flamelet models to non-premixed turbulent combustion a mixture fraction transport equation has to be solved in order to determine the statistical distribution of the laminar flamelets. One of the main advantages of the present model is that also this equation does not depend on the unity Lewis number assumption.

Although in this paper the model has been discussed in terms of steady diffusion flames, it also can be applied in unsteady turbulent non-premixed flow situations. The numerical implementation, as well as the choice of initial and boundary conditions, is very similar to conventional non-premixed flamelet models.

For numerical purposes the mixture fraction dependence of the scalar dissipation rate usually has to be approximated. From the analytic expressions given in the literature, Kim's formulation [31] is recommended here.

The constant species Lewis number approach has been shown to yield reasonable results, if the Lewis numbers of the chemical components are determined appropriately. Once the Lewis numbers are evaluated for a particular test case, they can be applied over a wide range of parameters for scalar dissipation rate, pressure, and boundary temperatures without loss of accuracy.

This research was supported by the European Commission in the frame of the JOULE III—Programme (JOF3-CT95-0003) and by the European Council for Automotive Research and Development (EUCAR) (Volkswagen and Volvo) within the DIESEL project.

REFERENCES

1. Liew, S. K., Bray, K. N. C., and Moss, J. B., *Combust. Flame* 56:199–213 (1984).
2. Müller, C. M., Breitbach, H., and Peters, N., *Twenty-Fifth Symposium (International) on Combustion*, The Combustion Institute, Pittsburgh, 1994, pp. 1099–1106.
3. Hollmann, C., and Gutheil, E., *Twenty-Sixth Symposium (International) on Combustion*, The Combustion Institute, Pittsburgh, 1996, to appear.
4. Pitsch, H., Wan, Y. P., and Peters, N., SAE Paper 952357, 1995.
5. Pitsch, H., Barths, H., and Peters, N., SAE Paper 962057, 1996.
6. Nandula, S. P., Brown, T. M., and Pitz, R. W., *Combust. Flame* 99:775–783 (1994).
7. Chen, Y. C., Mansour, M. S., and Peters, N., *Twenty-Sixth Symposium (International) on Combustion*, The Combustion Institute, Pittsburgh, 1996, to appear.
8. Peters, N., *Combust. Sci. Technol.* 30:1–17 (1983).
9. Peters, N., *Prog. Energy Combust. Sci.* 10:319–339 (1984).
10. Williams, F. A., *Combustion Theory*, 2nd ed., The Benjamin/Cummings Publishing Company, Menlo Park, CA, 1985 pp. 10, 73.
11. Menon, S., Calhoon, W. H., Goldin, G., and Kerstein, A. R., *Twenty-Fifth Symposium (International) on Combustion*, The Combustion Institute, Pittsburgh, 1994, pp. 1125–1131.
12. Law, C. K., and Chung, S. H., *Combust. Sci. Technol.* 29:129–145 (1982).
13. Im, H. G., Law, C. K., Kim, J. S., and Williams, F. A., *Combust. Flame* 100:21–30 (1995).
14. Seshadri, K., and Trevino, C., *Combust. Sci. Technol.* 64:243–261 (1995).
15. Cuenot, B., and Poinsot, T., *Combust. Flame* 104:111–137 (1996).
16. Barlow, R. S., and Chen, J.-Y., *Twenty-Fourth Symposium (International) on Combustion*, The Combustion Institute, Pittsburgh, 1992, pp. 231–237.
17. Haworth, D. C., Drake, M. C., Pope, S. B., and Blint, R. J., *Twenty-Second Symposium (International) on Combustion*, The Combustion Institute, Pittsburgh, 1988, pp. 589–597.
18. Peters, N., in *Reduced Kinetic Mechanisms for Applications in Combustion Systems* (N. Peters and B. Rogg, Eds.), Springer-Verlag, New York, 1993.
19. Mauss, F., Keller, D., and Peters, N., *Twenty-Third Symposium (International) on Combustion*, The Combustion Institute, Pittsburgh, 1990, pp. 693–698.
20. Bollig, M., Pitsch, H., Hewson, J. C., and Seshadri, K., *Twenty-Sixth Symposium (International) on Combustion*, The Combustion Institute, Pittsburgh, 1996, pp. 729–737.
21. Burke, S. D., and Schumann, T. E. W., *Ind. Eng. Chem.* 20:S.998 (1928).
22. Bilger, R. W., *Combust. Sci. Technol.* 13:S.155 (1976).
23. Bilger, R. W., *Twenty-Second Symposium (International) on Combustion*, The Combustion Institute, Pittsburgh, 1988, pp. 475–488.
24. Masri, A. R., and Bilger, R. W., *Comb. Flame* 73:261–285 (1988).
25. Smooke, M. D., Puri, I. K., and Seshadri, K., *Twenty-First Symposium (International) on Combustion*, The Combustion Institute, Pittsburgh, 1986, pp. 1783–1792.
26. Curtiss, C. F., and Hirschfelder, J. O., *J. Chem. Phys.* 17:550–555 (1949).
27. Coffee, T. P., and Heimerl, J. M., *Comb. Flame* 43:273–289 (1981).
28. Daguse, T., Croonenbroek, T., Rolon, J. C., Darabiha, N., and Soufiani, A., *Comb. Flame* 106:271–287 (1996).
29. Smooke, M. D., and Giovangigli, V., in *Reduced Kinetic Mechanisms and Asymptotic Approximations for Methane-Air Flames* M. D. Smooke, (Ed.), Springer-Verlag, New York, 1991 pp. 11, 16.
30. Effelsberg, E., and Peters, N., *Twenty-Second Symposium (International) on Combustion*, The Combustion Institute, Pittsburgh, 1988, pp. 693–700.
31. Kim, J. S., and Williams, F. A., *SIAM J. Appl. Math.* 53:1551–1566 (1993).

Received 18 March 1997; accepted date 30 August 1997